



EFFECTIVENESS OF BLADE FORWARD SWEEP IN A SMALL INDUSTRIAL TUBE-AXIAL FAN

Massimo MASI¹, Andrea LAZZARETTO²,
Stefano CASTEGNARO²

¹ *University of Padova, Department of Management and Engineering - DTG
stradella S. Nicola, 3. 36100 Vicenza, Italia*

² *University of Padova, Department of Industrial Engineering - DII
via Venezia, 1. 35131 Padova, Italia*

SUMMARY

Forward swept blades in low-speed axial fan rotors allow for appreciable gain in the stall margin and a small percentage gain in the maximum fan efficiency if the rotor blade circulation increases from the hub to tip. However, a reduction of the fan pressure at the design point counteracts these advantages. The paper investigates the effectiveness for small tube-axial fans of a design method suggested to increase the performance of an existing arbitrary vortex design by introducing the span-wise uniform distribution of blade forward sweep. The following three rotors for a 315-mm tube-axial fan have been tested: unswept, forward swept, and forward swept with additional sweep at the blade tip. Experimental data prove the effectiveness of the design method for these small fans.

INTRODUCTION

Adolf Busemann effectively conceived and explained the swept wings theory far in advance of the availability of the minimum knowledge and technology levels required for supersonic flight [1]. The application of sweep on turbomachine blades and the subsequent rigorous formalisation of the theoretical basis by Smith and Yeh [2] arrived later. Today, both high-speed compressors and low-speed axial fans massively use forward sweep (see, e.g., the applications reported in [3] for compressors and in [4] for highly loaded fans).

Focusing on the sweep applied to axial-flow fan rotors, the review [5] collects the findings of the main researchers on the topic. The introduction of forward sweep in the radial stacking line of rotor blades for low-speed axial fans allows an appreciable gain in the stall margin at the expense of a reduction of the fan pressure at the design point.

The same author recently observed [6] that several rotors featuring a blade circulation that increases from the hub to tip show a small percentage gain in the maximum fan efficiency, in contrast to free-vortex designs that appear unaffected in terms of maximum efficiency by the introduction of the blade sweep.

Accordingly, the literature on fans has suggested some methods that allow for including the sweep angle already in the preliminary design to limit the extensive experimental and/or Computational Fluid Dynamics (CFD) trial-and-error work required to find the distribution of the sweep angle that is best suited to a specific fan design. Among these methods, one of the first was proposed by [7], who suggested increasing the load selected for each aerofoil section of the preliminary unswept blade design accounting for the well-known unload due to the so-called $\cos(\lambda)$ effect [8]. Recently, [9] applied this suggestion and obtained interesting results in the design of a free-vortex rotor-straightener unit. Alternatively, [10] proposed a very complete method in which the effectiveness is assessed by the example reported in the paper itself, and the drawbacks, if any, require extensive CFD calculations.

A few years ago, the present authors proposed a method to increase either the performance [11] or the efficiency [12] of an existing arbitrary vortex design tube-axial fan by introducing a uniform radial distribution of blade forward sweep. According to the preliminary CFD calculations in [13], this method has allowed for an appreciable increase of the fan pressure at the design point without penalties in efficiency for a 560-mm tube-axial fan featuring a hub-to-tip ratio equal to 0.4. Moreover, the calculations have predicted a relevant increase of the maximum fan pressure if 6 degrees of additional forward sweep at the blade tip are superimposed to the distribution of sweep suggested by the method.

These promising predictions have not yet been supported by a specific experimental campaign. However, a partial support of the expected trends can be found in [14], where the authors presented experimental data and an extensive CFD analysis of a highly loaded fan rotor that they designed in both the unswept and forward swept configurations. In particular, the comparison shows that their design with a span-wise increasing distribution of blade forward sweep slightly improves the pressure of the unswept fan at the design point but reaches a very notable gain in peak pressure without strong decay in efficiency. However, the experimental results presented in [12] for a 315-mm tube-axial fan with hub-to-tip ratio equal to 0.44 and span-wise uniform blade forward sweep applied according to the described design method therein did not fully confirm the expected efficiency increase. In particular, they showed an increase of peak efficiency up to 5% without penalisation in fan pressure at blade positioning angles higher than the design, but they did not show the actual effectiveness of the applied sweep distribution at the design value of the blade positioning angle. The conservative values of both the forward sweep angle and Lieblein diffusion factor [15] distribution chosen for this design are likely the main reason for the not fully satisfactory results. The low values of the blade sections' Reynolds number might have played a relevant role as well.

This paper presents the results of the experimental tests performed on a 315-mm tube-axial fan similar to the fan analysed by CFD in [11] and [13] to assess the reliability of the reported design procedure and to verify whether the methodology is effective for fan rotors strongly affected by a low Reynolds number. To quantify the effects of the blade forward sweep on the performance and efficiency figures of this small fan, the following three different stacking lines of the rotor blades have been tested: unswept, forward swept, and forward swept with additional sweep at the blade tip.

THE 315-MM FAN DESIGN

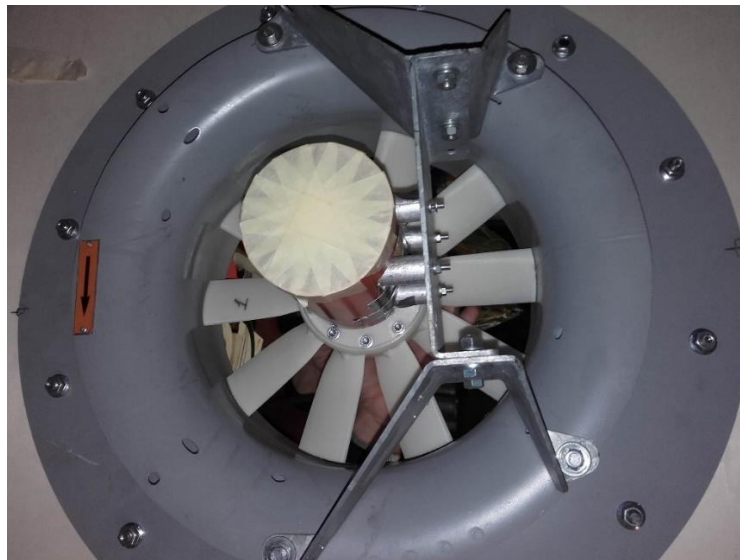
The three 315-mm tube-axial fans, described in the following subsections, differ from each other primarily in the blade stacking line. In particular, they feature a hub-to-tip ratio equal to 0.4 and a

tip clearance value that is typical of industrial fans. Table 1 reports the main features shared by the three fans.

Fan performance and efficiency at a specific flow rate q_v (or dimensionless flow rate coefficient $\Phi = q_v/(\omega D^3)$) will be expressed in the following text by fan pressure p_f (or dimensionless pressure coefficient $\Psi = p_f/(\omega D)^2$) and aerodynamic efficiency $\eta_{aer} = q_v p_f/(T\omega)$, where T is the shaft torque, and D and ω are the fan rotor diameter and rotational speed, respectively. Note that both fan pressure p_f and aerodynamic efficiency η_{aer} are defined in accordance with the ISO 5801:2008 standard (fan pressure p_{fA} and fan total efficiency η_{fA} , respectively).

Table 1: Main features of the 315-mm tube-axial fans.

Design Parameter		Value
Hub-to-tip ratio	ν	0.4
Outlet tangential velocity ratio	ε_S	$ca_2/ca_{avg} = 0.591$ (along the entire blade span)
Blade number	Z	10
Blade chord [mm]	l	51.2 (in the entire blade span – 47.8 at the hub)
Blade aspect ratio	B/l	1.81
Blade profile		F-Series (circular arc + C4 thickness distribution) [16]
Blade camber	θ	19.9° (before the inclusion of 2 % nose droop*)
Max. thickness-chord ratio	s/l	10 %
Tip clearance/blade span	t_c/B	1.61 %



*modification of the C4 camber line in the fore part of the aerofoil [16]

Unswep Fan: USW

The design condition chosen for this fan is equal to the one of an existing high-efficiency 560-mm tube-axial fan, which has been taken in [11] as CFD test case for the exploitation of the design

method suggested to increase the performance by the addition of a blade forward sweep. In particular, the dimensionless performance coefficients Φ and Ψ at the design condition are equal to 0.0906 and 0.0182, respectively. Note that, to minimise the design modifications required to obtain the forward swept rotor, the present unswept (USW) design slightly revises the unswept design originally suggested in [11] as the starting point of the method.

The aerofoil sections of the USW rotor blades were chosen based on the velocity triangles at six conical surfaces approximating the actual meridional flow in an annular cascade with the increase of the blade circulation from hub to tip. Span-wise distribution of the aerofoil stagger complies with the distribution chosen for the incidence angle i of the relative velocity at the inlet radius of the six conical surfaces.

Generally, each conical stream surface that crosses the blade passage intersects the rotor axis with a specific obliquity γ . In the USW design, the magnitude of the γ angle of each conical stream surface is assumed equal to the maximum obliquity value reached in the entire blade span according to the continuity constraint and the following assumptions:

- 1) Uniform and purely axial inlet velocity (i.e., inlet velocity ratio $ca_1/ca_{avg} = 1$);
- 2) Distribution of the outlet axial velocity ratio (i.e., $\Sigma a = ca_2/ca_{avg}$) in accordance with the radial equilibrium of a flow with span-wise constant tangential velocity ratio (i.e., $\varepsilon_S = ca_2/ca_{avg}$).

To obtain a quasi-constant swirl design (i.e., $\varepsilon_S \approx \text{const}$), the same aerofoil section and the same chord length l have been applied along the entire blade span. Thus, a span-wise constant value of the incidence angle i leads to a constant value of the aerofoil lift coefficient C_L and allows for the uniform distribution of the blade load lC_L (if the mutual interference factor is neglected).

Table 2: Geometric and kinematic parameters of the USW blading.

Parameters	Values					
	1 (root)	2	3	4	5	6 (tip)
Section ID						
Dimensionless radius x	0.402	0.500	0.598	0.696	0.843	0.990
Section obliquity γ	16.8°	16.8°	16.8°	16.8°	16.8°	16.8°
Rotor inlet dimensionless radius x_{in}	0.371	0.470	0.567	0.666	0.813	0.960
Rotor exit dimensionless radius x_{out}	0.432	0.531	0.628	0.727	0.874	1.021
Rotor exit axial velocity ratio Σa	0.527	0.703	0.857	0.996	1.184	1.353
Solidity σ	1.20	1.03	0.87	0.74	0.61	0.52
Stagger ξ	47.3°	53.5°	58.0°	61.4°	65.2°	67.9°

The final blade was obtained by stacking the aerofoil planform positioned and staggered on each cylindrical surface along a radial line that intersects the cone approximating the corresponding actual stream surface at 45% of the chord length. Table 2 reports the geometric and kinematic parameters of the USW blading.

Note that staggering aerofoil planforms on cylindrical surfaces instead of conical surfaces leads to stagger angles that are lower than those required by the design. Accordingly, the effective local

incidence and the blade load along the entire blade span are higher than the design. On the other hand, the camber of the profile “seen” by the bulk flow (i.e., the camber obtained from the intersection of each pseudo-conical stream surface and the blade) is lower than the camber of the chosen aerofoil planform. This reduction of the effective camber unloads the blade at design condition. In the design phase, it was assumed that these two counteracting effects compensate each other. However, the difference between the stagger angle in the design and the effective stagger is almost negligible.

Forward Swept Fan: FSW

The uniformly swept rotor was designed according to the method that allowed obtaining the forward swept version of the 560-mm tube-axial studied by CFD in [11]. The reference reports all the details of the design method, whereas [17] presents and discusses its theoretical basis. Since the original method was conceived for application on an already existing arbitrary vortex design fan, only the final objective of the method is recalled. This can be summarised by the following statement: *The distribution of sweep angle that allows for the maximum fan pressure at the design operation for a given distribution of the blade load is the one corresponding to a blade stacking line where the chosen aerofoil sections ‘see’ a quasi-two-dimensional flow.*

According to this statement, different load distributions require different sweep distributions and, in general, the higher the positive circulation gradient along the blade span, the higher the forward sweep λ . Thus, a free-vortex design to obtain the maximum fan pressure from a specific selection of aerofoil sections should feature a radial stacking line.

To obtain the uniformly swept blade (FSW) from the USW one, it is necessary to:

- 1) Restore the position of each aerofoil on the conical surface where it should be placed in strict accordance to the preliminary design step of the USW rotor.
- 2) Move each section upstream along the helicoidal path identified by the conformal mapping of the aerofoil chord on the cylindrical surface passing at 45% of the chord length, until the stacking line of the resulting blade becomes forward swept by an angle $\lambda = \gamma$.

The limited increase of blade circulation in the span-wise direction expected for common industrial tube-axial fans leads to a limited radial shift of the meridional flow (outside the boundary layer). Accordingly, the amount of forward sweep suggested by the method for the FSW rotor is limited as well ($\lambda = 16.8^\circ$ in the present case). At a glance, this could lead to some concerns on the reliability of the design method, as the sweep angle suggested for the recent and past designs of fan rotors is appreciably high (e.g., on the order of $40 \div 60^\circ$ in [7, 9]). It is worth noting that those high levels of forward sweep were aimed mainly at fan noise reduction, as clearly stated in [9], whereas the present FSW design focuses on performance and efficiency but disregards any aspect related to noise emission.

Forward Swept Fan with Non-Uniform Distribution of Blade Sweep: FSW+6tip

Finally, an increased amount of forward sweep has been added close to the tip of the FSW blade. In particular, the profile section at the blade tip (Section 6 in Tab. 1) was moved upstream along the same helicoidal path previously used as rail to obtain the FSW blade from the USW blade. Figure 1 qualitatively sketches the FSW blade and its six skeleton aerofoils in black. The forward or backward motion of the outermost aerofoil along the blue broken line path allows including an additional forward or backward sweep at the blade tip shown by the red and green parts, respectively.

The FSW+6tip blade includes 6 degrees of additional forward sweep and was obtained by a ‘loft’ operation, which enveloped all the sections and allowed for a smooth change of the sweep angle towards the blade tip. This design should increase Ψ and η_{aer} at peak pressure operation without

penalties in the entire Φ range from the design point to free delivery, according to the results of the preliminary CFD calculations [13] performed on a forward swept rotor (perfectly similar to the FSW) modified at the blade tip by inclusion of different amounts of sweep.

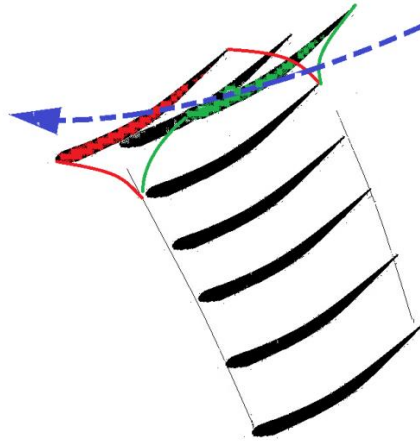


Figure 1: Qualitative sketch of the FSW blade (black) and its modified version with addition of forward sweep (red) or backward sweep (green) at the blade tip by motion of the outermost aerofoil along the direction fixed by conformal mapping of its chord on the supporting cylindrical surface (blue broken line).

Summary

For the sake of immediate comparison, Fig. 2 collects the front and rear views of all three 315-mm rotors described in the previous subsections. All three rotors feature a tip clearance that is strictly similar to that of the corresponding 560-mm rotors in [13]. However, FSW and FSW+6tip rotors are a perfectly scaled copy of those in [13], whereas the present USW rotor blades are not identical in shape to the 560-mm USW. In fact, the two USW design approaches differ from each other in the choice of the stream surface shape assumed to support the peripheral velocity vector of the velocity triangles at the leading and trailing edges of each section of the rotor blade. In particular, both the designs account for the radial shift of the meridional flow, but the inlet and outlet velocity triangles of each blade section are assumed to be supported by a unique cylindrical surface in [13] and by two cylindrical surfaces of different radii in the present USW design.

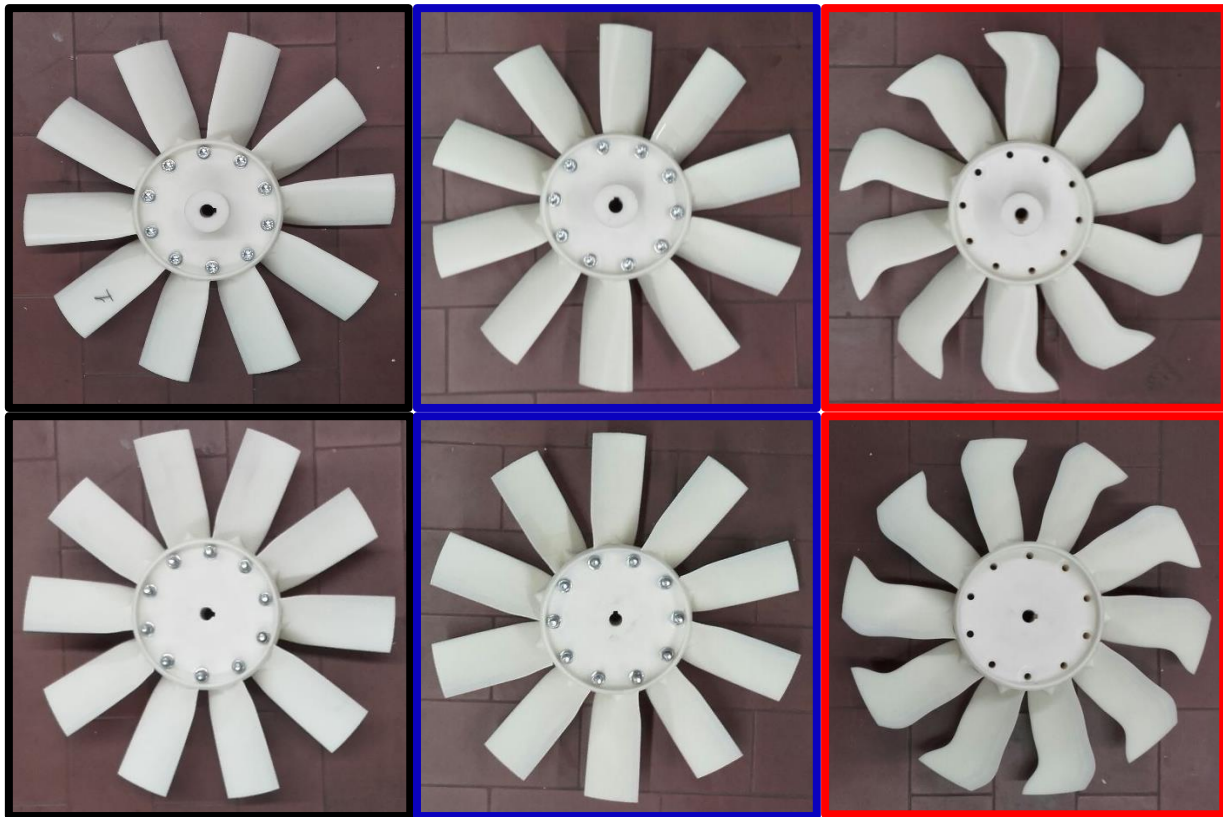


Figure 2: USW, FSW, and FSW+6tip 315mm rotors (from left to right) - front view (above) – rear view (below).

To conclude the description of the 315-mm rotor prototypes, Fig. 3 shows the global performance parameters predicted by the preliminary CFD calculations performed in [13] on the three 560-mm tube-axial fans. At design operation ($\Phi = 0.0906$), the aerodynamic efficiency predicted for the USW fan is $\eta_{aer} = 0.62$, and the corresponding pressure coefficient Ψ reaches a value of about 0.021 (i.e., well above the pressure coefficient of the reference existing fan).

As global trends, these preliminary calculations of constant-swirl design rotor blades suggest that:

- 1) the inclusion of a span-wise uniform forward sweep (i.e., the FSW rotor) allows for,
 - a. an increase of the pressure coefficient Ψ in the entire fan operation range, keeping the aerodynamic efficiency η_{aer} unchanged at flow rates ranging from peak pressure to free delivery;
 - b. an increase in the stall margin.
- 2) the inclusion of 6 degrees of additional forward sweep at the tip of the FSW blade (i.e., the FSW+6tip rotor) allows for,
 - a. a progressive increase of both Ψ and η_{aer} in the operation range from peak pressure to stall;
 - b. a progressive very slight decrease of Ψ in the flow rate range from maximum η_{aer} to free delivery, likely without relevant modifications in η_{aer} values.

Since all the fans run at the same rotational speed, the blade Reynolds number for the 560-mm fans studied by CFD is about four times higher than that for the present 315-mm prototypes. Accordingly, it is expected that both Ψ and η_{aer} curves of the small prototypes exhibit some differences in the behaviours just summarised. This occurrence and the limited accuracy of the preliminary CFD calculations (discussed in [13]) prompt the experimental tests presented in the following text, aimed at verifying the effectiveness of the design method for small industrial fans.

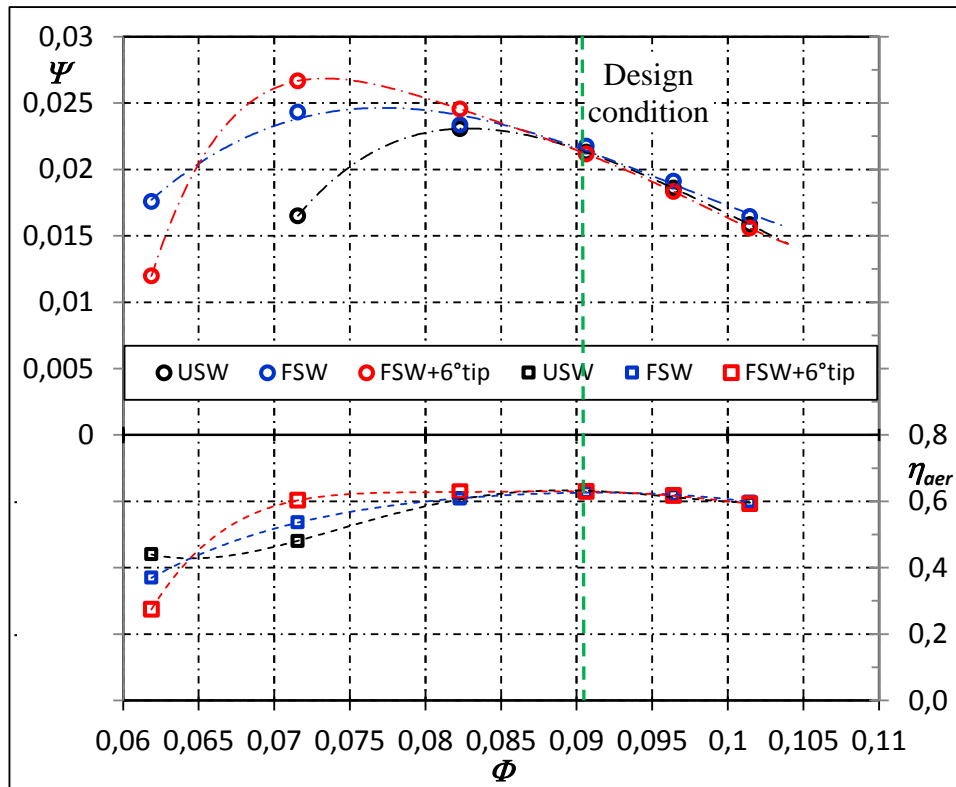


Figure 3: CFD predictions in black, blue, and red, respectively, for USW, FSW, and FSW+6°tip 560-mm fans (adapted from [13]).

EXPERIMENTAL FACILITY

Fan Prototypes

The three series of blades (i.e., the *USW*, *FSW*, and *FSW+6°tip*) have been manufactured in Acrylonitrile Butadiene Styrene (ABS) plastic with a rapid-prototyping technique. The dimensional uncertainty declared by the manufacturer is 0.1 mm on the chord length and 0.25 mm on the blade height. The minimum feasible dimension is 0.2 mm. No dimensional differences have been measured with respect to the nominal dimensions, however. Blades and rotor boss are manufactured separately and subsequently assembled to allow for the test of performance at several blade positioning angles. The surface roughness has been repeatedly measured, providing Ra equal to 18.6 μm and 11.4 μm in span-wise and chordwise directions, respectively.

Experimental Apparatus

The experimental tests have been performed at the large test rig installed in the *Laboratorio di Macchine Termiche e Aeraliche* of the University of Padova (see Fig. 4).



Figure 4: Inlet chamber test rig used for the tests. The picture was taken during the FSW test.

The rig has been designed and built according to the Type 3 inlet-chamber configuration included in the ISO 5801:2008 standard. A multi-nozzle system and a pitot tube allow for the measurements of the flow-rate and the air total pressure inside the chamber, respectively. The full description of the rig is reported in [18]. The direct measure of the shaft torque is performed during the tests using the torque-table dynamometer visible in Fig. 2. In accordance with ISO 5801:2008, fan aerodynamic torque is derived by subtraction from the shaft torque of power losses due to the ball-bearings and transmission belt. These latter are measured at the end of each test, removing the fan rotor and running the system at the same rotational speed set for the performance test just completed. All tests have been performed according to the simplified procedure of the ISO standard for $Ma_{2ref} < 0.15$ and pressure ratio lower than 1.02 because the fan rotational speed was about 1530 rpm. The instrumentation and the estimated absolute uncertainty are reported in Tab. 3.

Table 3: Instruments and estimated accuracy.

Instruments	Accuracy
Water micromanometers	$\pm 0.05 \text{ mm H}_2\text{O}$
Rpm counter	$\pm 2 \text{ rpm}$
Torque-table weight distance	$\pm 3 \text{ mm}$
Digital mass scale	$\pm 1 \text{ g}$
Wet-dry bulb thermometer	$\pm 0.5 \text{ K}$
Digital barometer	$\pm 100 \text{ Pa}$
Digital thermometer	$\pm 0.1 \text{ K}$

Uncertainty Estimation on the Results

The measurements uncertainty for mass flow rate q_m , fan pressure p_f , and aeraulic efficiency η_{aer} , are reported in Tab. 4. They have been estimated according to the ISO standards 5801:2008 (pp. 64-65) and 5167-1 (p. 18) at the best efficiency point.

Table 4: Measurement uncertainty.

	u_{q_m} (%)	u_{p_f} (%)	$u_{\eta_{aer}}$ (%)
Peak Efficiency	1.26	0.94	1.97

RESULTS

Figure 5 shows the dimensionless fan pressure rise Ψ (filled circle markers) and the aeraulic efficiency η_{aer} (filled square markers) curves measured for all the three 315-mm tube-axial fans. The experimental data for the FSW and FSW+6tip fans have been measured for the blade positioning angle value that allows obtaining their best η_{aer} at the same Φ of the USW fan's best efficiency point, with this latter being equal to about 22 degrees.

First, it is apparent that the fan pressure coefficient of the USW fan at the design condition notably exceeds either the CFD estimate for the similar 560-mm diameter fan (~ 0.024 against ~ 0.021 or about +14 %) or the experimental datum for the existing 560-mm tube-axial fan (~ 0.024 against ~ 0.018 or about +33 %). Since these Ψ values are quite high for tube-axial fans and η_{aer} does not seem compromised by this, it is concluded that a not very sophisticated blade design approach coupled with the adoption of the F-Series aerofoil sections suggested by Wallis [16] is still a very attractive tool for the effective design of small industrial fans.

That said, the η_{aer} curve of the three 315-mm prototypes shows that both the overall trend and the best efficiency flow rate are not affected by the difference in the shape of these blades. To a lesser extent, this is valid for the efficiency values as well, as will be discussed later.

The comparison between USW and FSW data (i.e., black and blue coloured data in Fig. 5) shows a FSW pressure curve appreciably higher than the USW curve in the entire stable operation range of the fan. This advantage does not cause any decrease of the fan aeraulic efficiency. In particular, the FSW blade allows for ~ 2 % gain in fan pressure of the USW blade at the best efficiency point. The higher the fan flow rate, the higher the gain. Alternatively, the level of forward sweep suggested by the design method does not lead to the expected improvement of the fan stall margin that remains equal to $\sim 17\%$ of the design flow rate.

The additional sweep at the blade tip featured by the FSW+6tip rotor (red coloured data in Fig. 4) notably increases the fan pressure coefficient featured by the FSW fan from the best efficiency duty to incipient stall flow rate. At the best aeraulic efficiency point, the FSW fan pressure increases by ~ 2 %. This leads to an overall pressure increase due to the forward sweeping the USW blade equal to ~ 4 % ($\Psi \approx 0.025$ and 0.024 for FSW+6tip and USW rotor, respectively). The fan pressure increase is higher than 7 % at the USW peak pressure flow rate (value of ~ 0.029 against ~ 0.027 for the FSW+6tip and USW fan pressure coefficients). Moreover, Φ at peak pressure reduces from ~ 0.075 to ~ 0.066 . This leads to a percentage increase of the fan stall margin on the order of ~ 60 % (~ 27 % for FSW+6tip against ~ 17 % for either the USW or FSW fan).

The aeraulic efficiency at the best efficiency point increases by ~ 1.5 %, passing from the USW to the FSW rotor and from the FSW to the FSW+6tip. However, these differences are lower than experimental uncertainty. Accordingly, it should be concluded that the FSW fan features a maximum η_{aer} equal to the USW fan, whereas the FSW+6tip certainly allows for an improvement of the USW aeraulic efficiency by a small percent. A better η_{aer} for the FSW+6tip fan is apparent at flow rate coefficients ranging from the best efficiency point to throttling.

Apart from the differences in efficiency magnitude between CFD and experiments, Fig. 6 shows that the maximum efficiency of the three prototypes shifts towards lower flow rates when compared to that calculated for the 560-mm fans. The Reynolds effect certainly plays a role in this because it

is expected that the lower the Reynolds number (i.e. the size in this case), the lower the peak efficiency flow coefficient. Nonetheless, examining the comparison, this effect seems quite limited, although this and other discussions related to experimental data and CFD results reported in Fig. 6 should account for the effects of the limited accuracy of the CFD calculations discussed previously.

However, there are elements to suppose that the three prototypes are able to reach higher efficiency at a higher flow rate if manufactured in a larger size.

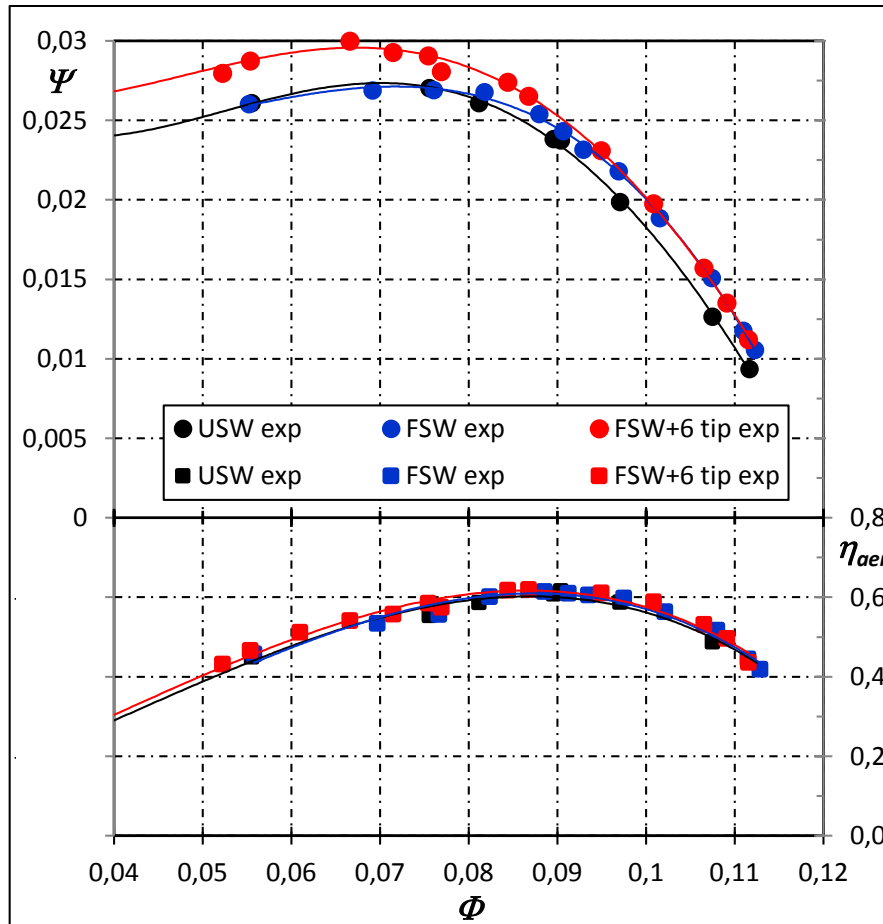


Figure 5: Fan pressure coefficient and aerodynamic efficiency against the flow rate coefficient measured for USW, FSW, and FSW+6tip 315-mm fans.

CONCLUSION

The experimental test performed to verify the effect of different distributions of blade forward sweep on pressure and aerodynamic efficiency curves for three 315-mm tube-axial fans has confirmed the effectiveness of the criterion. These fans were designed in accordance with an easy-to-use criterion suggested by the authors to increase fan performance by inclusion of a proper level of forward sweep on constant-swirl designed rotors.

Most of the trends shown by simplified preliminary CFD analyses on the full-scale fans were reproduced by the experiments and, in particular:

- Span-wise uniform forward sweep of constant swirl design blades,
 - increases fan pressure featured by the unswept design at maximum aerodynamic efficiency operation by more than 2% without reduction of efficiency;
 - improves the fan pressure of the unswept design in the entire stable operation range by a percentage that increases from peak pressure towards free-delivery operation;
 - does not increase the stall margin of the unswept design;

- does not worsen the aerodynamic efficiency of the unswept design in the entire flow rate range from shutoff to free delivery.
- Uniformly swept blades featuring 6 degrees of additional sweep close to the tip,
 - appreciably increase the fan pressure of the uniformly swept design at flow rates lower than the design point (by about 10% at peak pressure operation) without penalties in aerodynamic efficiency;
 - increase the stall margin of both the uniformly swept and unswept designs;
 - slightly increase the aerodynamic efficiency of the uniformly swept design in the entire operation range, especially at flow rates lower than the peak pressure duty (by about 2%).

Finally, it is likely that the criterion used to include the forward sweep in the preliminary design of constant swirl blades, which proved experimentally to be beneficial for small tube-axial fans, could be even more effective, if applied to industrial fans of larger size, considering the expected lower efficiency (and performance) of turbomachines operating in low Reynolds number conditions.

BIBLIOGRAPHY

- [1] J. D. Anderson – *A History of Aerodynamics and Its Impact on Flying Machines*. Cambridge University Press, New York, **1997**
- [2] L. M. Smith, H. Yeh – *Sweep and dihedral effects in axial-flow turbomachinery*. ASME J. Basic Eng., 85, 401-416, **1963**
- [3] A. R. Wadia, P. N. Szucs, D. W. Crall – *Inner working of aerodynamic sweep*. ASME paper 97-GT-401, **1997**
- [4] K. Mohammed, D. Prithvi Raj – *Investigations on Axial Flow Fan Impellers with Forward Swept Blades*. ASME Paper No. 77-FE-1, **1977**
- [5] J. Vad – *Aerodynamic effects of blade sweep and skew in low-speed axial flow rotors at the design flow rate: an overview*. Proc. IMechE, Part A: J. Power and Energy, 222, 69-85, **2008**
- [6] J. Vad, G. Halász, T. Benedek – *Efficiency gain of low-speed axial flow rotors due to forward sweep*. Proc. IMechE, Part A: J. Power and Energy, Technical Note 0(0), 1-8, **2014**
- [7] M. G. Beiler, T. H. Carolus – *Computation and measurement of the flow in axial flow fans with skewed blades*. ASME J. Turbomachinery, 121, 59-66, **1999**
- [8] R. T. Jones – *Wing Theory*, Princeton Legacy Library, **1990**
- [9] D. Giesecke, J. Friedrichs, U. Stark, M. Dierks – *Aerodynamic and Acoustic Performance of a Single Stage Axial Fan With Extensive Blade Sweep Designed to Limit Noise Emissions*. ASME Paper GT2016-56555, **2016**
- [10] J. Vad – *Incorporation of forward blade sweep in preliminary controlled vortex design of axial flow rotors*. Proc. IMechE, Part A: J. Power and Energy, 226, 462-478, **2012**
- [11] M. Masi, M. Piva, A. Lazzaretto – *Design guidelines to increase the performance of a rotor-only axial fan with constant-swirl blading*. ASME paper GT2014-27176, **2014**
- [12] M. Masi, S. Castegnaro, A. Lazzaretto – *Forward sweep to improve the efficiency of rotor-only tube-axial fans with controlled vortex design blades*. Proc. IMechE, Part A: J. Power and Energy, 230, issue: 5, 512-520, **2016**
- [13] M. Masi, A. Lazzaretto – *Preliminary investigation on the effect of the modification of the sweep angle at the blade tip of forward swept axial fans*. ASME paper GT2017-63795, **2017**

- [14] A. Corsini, F. Rispoli – *Using sweep to extend the stall-free operational range in axial fan rotors*. Proc. IMechE, Part A: J. Power and Energy, 218, 129-139, **2004**
- [15] S. Lieblein, F. C. Schwenk, R. L. Broderick – *Diffusion factor for estimating losses and limiting blade loadings in axial-flow-compressor blade elements*. NACA-RM-E53D01, **1953**
- [16] R.A. Wallis – *The F-Series airfoils for fan blade sections*, Mech. Eng. Trans. I. E. Aust., ME2 (1), 12-20, **1977**
- [17] M. Masi, A. Lazzaletto – *A simplified theory to justify forward sweep in low hub-to-tip ratio axial fan*. ASME paper GT2015-43029, **2015**
- [18] S. Castegnaro, M. Masi, A. Lazzaletto – *Design and testing of an ISO 5801 inlet chamber test rig and related issues with the Standard*. Proc. Fan 2018 Conference, **2018**.